ORIGINAL RESEARCH PAPER

Fuel Cells DOI: 10.1002/fuce.201300054

Synthesis and Characterization of a New Fluorine-Containing Polybenzimidazole (PBI) for Proton-Conducting Membranes in Fuel Cells

X. Li[1], G. Qian[1], X. Chen[2], B. C. Benicewicz[1]*

[1] Department of Chemistry and Biochemistry, University of South Carolina, Columbia, SC 29208, USA
[2] Department of Chemical Engineering, University of South Carolina, Columbia, SC 29208, USA

Received February 25, 2013; accepted May 21, 2013; published online August 30, 2013

Abstract

A new type of fluorine-containing polybenzimidazole, namely poly(2,2′-(2,2′-bis(trifluoromethyl)-4,4′-biphenylene)-5,5′-bibenzimidazole) (BTBP-PBI), was developed as a candidate for proton-conducting membranes in fuel cells. Polymerization conditions were experimentally investigated to achieve high molecular weight polymers with an inherent viscosity (IV) up to 1.60 dl g^{-1}. The introduction of the highly twisted 2,2′-disubstituted biphenyl moiety into the polymer backbone suppressed the polymer chain packing efficiency and improved polymer solubility in certain polar organic solvents. The polymer also exhibited excellent thermal and oxidative stability. Phosphoric acid (PA)-doped BTBP-PBI membranes were prepared by the conventional acid imbibing procedure and their corresponding properties such as mechanical properties and proton conductivity were carefully studied. The maximum membrane proton conductivity was approximately 0.02 S cm^{-1} at 180 °C with a PA doping level of 7.08 PA/RU. The fuel cell performance of BTBP-PBI membranes was also evaluated in membrane electrode assemblies (MEA) in single cells at elevated temperatures. The testing results showed reliable performance at 180 °C and confirmed the material as a candidate for high-temperature polymer electrolyte membrane fuel cell (PEMFC) applications.

Keywords: Eaton's Reagent, Fluorinated Polybenzimidazole (PBI), Fuel Cell, High Temperature Polymer Electrolyte Membrane, PEMFC, Phosphoric Acid

1 Introduction

Polybenzimidazoles (PBI) are a class of heterocyclic polymers, which have exceptional thermal, chemical, and mechanical stabilities at elevated temperatures. When fabricated into membranes and doped with low vapor pressure proton conductors such as phosphoric acid (PA), the corresponding acid-doped PBI membranes were reported as promising alternatives to traditional perfluorosulfonic acid type membranes (e.g. Nafion®). For the application of polymer electrolyte membrane fuel cells (PEMFCs) such membranes provide benefits such as high operational temperatures (120–200 °C), fast electrode kinetics, simplified water management, and high tolerance to fuel impurities (e.g. CO, H_2S) [1–5]. Among various PBI derivatives, *meta*-PBI (poly(2,2′-(m-phenylene)-5,5′-bibenzimidazole)) is the most studied due to its commercial availability, but it also has weaknesses such as weak mechanical properties at high acid loading and poor solubility in organic solvents. Another important PBI variant is *para*-PBI (poly(2,2′-(*p*-phenylene)-5,5′-bibenzimidazole)). Its acid-doped membrane was prepared by a special sol–gel process and exhibited higher acid doping levels (>30 mol PA per PBI repeat unit) and better proton conductivity (>0.2 S cm^{-1}) than *meta*-PBI while still maintaining robust mechanical strength [3, 6]. However, the stiff chain characteristic of *para*-PBI caused by a more rigid *para*-oriented moiety makes the polymer virtually insoluble in any organic solvents, which limits its processing window. Therefore, in recent years considerable research has been focused on investigating new PBI chemistry, which could offer a better combination of desired properties for fuel cell applications.

[*] *Corresponding author, benice@sc.edu*

One effective way to improve the performance of polymers is to introduce fluorine or fluorine-containing groups (e.g. trifluoromethyl group (–CF_3)) into the polymer structure [7, 8]. This strategy has been widely used in the structural modifications of high-performance polymers such as polyimides, polyamides and poly(arylene ether)s and the respective polymers show good solubility in organic solvents, low water uptake and dielectric properties, and high thermal and oxidative stability [9–13]. Some partially fluorinated PBIs such as 4F-PBI, 6F-PBI, and PFCB-PBI have already been synthesized and exhibited better solubility, thermal and oxidative stability than non-fluorinated PBIs [14–16]. When assessing novel fluorine-containing structures, a special group that had not been previously investigated was the 2,2′-bistrifluoromethyl-4,4′-biphenylene moiety. It is well known that the steric repulsion of trifluoromethyl groups at the 2 and 2′ position of the biphenyl group will force the nonplanarity of the two phenyl rings while simultaneously maintaining the rigid rod-like backbone [17]. This specific conformation was reported to be able to largely suppress the close chain packing of polymer backbones and improve the polymer's solubility and other properties [17–19]. In this work, a novel fluorine-containing PBI (BTBP-PBI) has been successfully synthesized from 3,3′,4,4′-tetraaminobiphenyl and 2,2′-bis(trifluoromethyl)-4,4′-biphenyldicarboxylic acid by solution polymerization in Eaton's reagent [20]. Polymerization conditions were investigated to achieve high molecular weight polymers. Commercial *meta*-PBI and partially fluorinated 6F-PBI containing similar functional groups (–CF_3) as BTBP-PBI were also synthesized in this work for detailed comparisons [14, 21]. All the polymers were fully characterized by FTIR, ^{1}H NMR, ^{19}F NMR, TGA, WAXS and other techniques. PA-doped PBI membranes were prepared *via* traditional PA imbibing procedures and the acid doping behavior, mechanical properties, and proton conductivity of the membrane were studied. The PBI membranes were also fabricated into membrane electrode assemblies (MEA) and tested under various conditions to evaluate its fuel cell performance.

2 Experimental Methods

2.1 Materials

2,2′-Bis(trifluoromethyl)benzidine (98.5%) was purchased from Akron Polymer Systems. 3,3′,4,4′-Tetraaminobiphenyl (TAB, polymer grade, ~97.5%) was donated by Celanese Ventures, GmbH (now, BASF Fuel Cell). Polyphosphoric acid (PPA, 115%) was purchased from Aldrich Chemical Co. All other reagents (e.g. sodium cyanide, sodium nitrite, copper cyanide, etc.) and solvents (e.g. *N*,*N*-dimethylacetamide, 1-methyl-2-pyrrolidinone, ammonium hydroxide, etc.) were purchased from Fisher Scientific. Unless otherwise specified, all chemicals were used without further purification.

2.2 Monomer and Polymer Synthesis

2.2.1 Synthesis of 2,2′-Bis(trifluoromethyl)-4,4′-biphenyldicarbonitrile (2)

To a 500 ml round-bottom flask, 2,2′-bis(trifluoromethyl)-benzidine (16.012 g, 50 mmol), hydrochloric acid (41.6 ml, 12.1 M), and water (100 ml) were added. The mixture was then heated at approximately 100 °C for 20–30 min until the solution became clear and developed a light orange color. The following operations were all conducted in an ice bath (0–5 °C) unless otherwise noted. A solution of sodium nitrite (8.624 g, 125 mmol) in 100 ml water was added dropwise to the above-mentioned ammonium salt solution to obtain an orange color solution. The reaction mixture was stirred for 1 h, and then neutralized by sodium bicarbonate solution until pH was 7. To a 500 ml beaker, copper cyanide (11.195 g, 125 mmol), sodium cyanide (18.378 g, 375 mmol), and water (100 ml) were added to obtain a clear solution. The diazonium salt solution was then gradually added to the cyanating reagent solution with vigorous mechanical stirring. The light brown precipitate that formed was collected by filtration and sublimated under vacuum at 130 °C to obtain white crystals (4.901 g, yield 25.6%). ^{1}H NMR (400 Hz, DMSO-d_6): 7.684(d, J = 8, 2H, Ar–**H**), 8.262 (dd, $J_{1,2} = J_{3,4} = 1.6$, $J_{1,3} = J_{2,4} = 8$, 2H, Ar–**H**), and 8.494 (d, J = 1.2, 2H, Ar–**H**). ^{13}C NMR (400 Hz, DMSO-d_6): 113.379, 117.590, 121.779, 124.504, 130.913, 132.912, 136.157, 140.192. Elemental Analysis for $C_{16}H_6N_2F_6$: C, 56.48; H, 1.78; N, 8.23; F, 33.50. Found: C, 56.49; H, 1.70; N, 8.23; F, 33.13.

2.2.2 Synthesis of 2,2′-Bis(trifluoromethyl)-4,4′-biphenyldicarboxylic Acid (3)

The dicarboxylic acid was synthesized following the procedures in the literature [22]. To a 100 ml round-bottom flask, 2,2′-bis(trifluoromethyl)-4,4′-biphenyldicarbonitrile (2.722 g, 8 mmol), potassium hydroxide (2.016 g, 36 mmol), ethylene glycol (18 ml) and water (1 ml) were added. The mixture was heated to reflux overnight. After refluxing, vacuum distillation was performed to the light yellow solution to remove some solvent (>10 ml). When the solution was cooled to room temperature, the white precipitate formed was collected by filtration and then dissolved in approximately 250 ml water. The solution was filtered again to remove undissolved byproduct and acidified by concentrated hydrochloric acid (12 M) until pH=1. The white precipitate was collected by filtration and dried at 110 °C overnight to obtain the final product in 82.7% yield. ^{1}H NMR (400 Hz, DMSO-d_6): 7.566 (d, J = 8, 2H, Ar–**H**), 8.240 (dd, $J_{1,2} = J_{3,4} = 1.6$, $J_{1,3} = J_{2,4} = 8$, 2H, Ar–**H**), 8.286 (d, J = 1.2, 2H, Ar–**H**), and 13.663 (b, 2H, COO**H**). ^{13}C NMR (400 Hz, DMSO-d_6): 122.378, 125.102, 126.894, 132.164, 132.525, 132.699, 140.411, 166.126. Elemental Analysis for $C_{16}H_8O_4F_6$: C, 50.81; H, 2.13; F, 30.14. Found: C, 50.71; H, 2.01; F, 29.86.

2.2.3 Synthesis of PBI Polymers

The general synthetic procedure of BTBP-PBI is described as follows. A 100 ml, three-necked, round-bottom flask was

fitted with an overhead mechanical stirrer and nitrogen inlet and outlet. Eaton's reagent (PPMA, phosphorous pentoxide: methanesulfonic acid = 1: 10, w:w) was prepared according to the literature [20]. 2,2′-Bis(trifluoromethyl)-4,4′-biphenyldicarboxylic acid (1.135 g, 3 mmol) and TAB (0.643 g, 3 mmol) were added to the reactor in a nitrogen glove box, followed by the addition of 12–20 ml of PPMA. The reaction mixture was then stirred by the mechanical stirrer at 55 rpm and purged with slow nitrogen flow. The reaction temperature was controlled by a programmable temperature controller with ramp and soak capabilities. The typical final polymerization temperatures were 140 °C for 30–40 h. As the reaction proceeded, the solution became more viscous and developed a dark brown color. At the end of the polymerization, the polymer solution was poured into water, pulverized, neutralized with ammonium hydroxide, and vacuum dried at 110 °C overnight to obtain the polymer powders. The general synthetic procedure of *meta*-PBI and 6F-PBI is similar as that of BTBP-PBI. The detailed polymerization conditions can be found in literature [14, 21].

2.3 PA-Doped PBI Membrane Preparation

To a 50 ml round bottom flask, BTBP-PBI powders (0.500 g) and *N*,*N*-dimethylacetamide (DMAc, 33 ml) were mixed and then refluxed (oil bath temperature 180 °C) for 2–3 h until most polymers were dissolved. After refluxing, the undissolved or swollen polymers were removed by centrifugation at 5000 rpm for 0.5 h to obtain a clear PBI solution. Dense PBI films were prepared by solution casting under dry nitrogen atmosphere. The PBI solution was slowly poured onto a clean glass plate, which was taped with glass slides on each side to restrain the movement of solution. After casting, the wet-film was dried slowly under nitrogen at approximately 40 °C (hot-plate temperature) to remove most solvent. Then the film was transferred to the vacuum oven and heated at 110 °C overnight to obtain the PBI dense membranes. The PA-doped BTBP-PBI membrane was obtained by immersing the PBI dense membrane into PA solution with respective concentrations for more than 48 h. The PA-doped *meta*-PBI and 6F-PBI membranes were prepared following similar procedures.

2.4 Characterization

2.4.1 Monomer and Polymer Characterization

^{1}H NMR, ^{13}C NMR, and ^{19}F NMR spectra were recorded on a Varian Mercury 400 spectrometer. FTIR spectra were recorded on a PerkinElmer Spectrum 100 FT-IR spectrometer with a three-reflection diamond/ZnSe crystal. The inherent viscosities (IV's) of the polymer samples were measured with a Cannon Ubbelohde viscometer at a polymer concentration of 0.2 g dl^{-1} in concentrated sulfuric acid (96 wt.%) at 30 °C. Thermogravimetric analysis (TGA) thermograms were obtained using TA Q5000 IR Thermogravimetric Analyzer at a heating rate of 10 °C min^{-1} under nitrogen flow (20 ml min^{-1}). The solubility of PBIs was evaluated at ambient temperature. The PBI powders were mixed with respective solvent and shaken on a wrist action shaker for more than 48 h. Oxidative stability was studied based on dry polymer powders by Fenton's test. Fenton's reagent (20 ppm Fe(II) in 3% H_2O_2) is a very effective method to generate hydroxyl/peroxyl radicals. The polymer powders were predried in oven at 110 °C overnight and weighed. Then they were placed into Fenton's reagent at r.t. and 80 °C for 24 h. After that, the samples were filtered, washed with water and dried in the oven at 110 °C for 24 h to obtain the final weight.

2.4.2 Membrane Characterization

The wide-angle X-ray diffraction (WAXD) was measured on a Rigaku MiniFlexll Desktop X-ray Diffractometer with the Cu-Kalpha (lamda = 1.5419 anstrom) radiation. The data were recorded in the 2theta range from 3 to 45 degree at a rate of 2-degree per minute. The tensile properties of the BTBP-PBI membranes were measured by TA RSA III Solid Analyzer at a constant Hencky strain rate of 0.001 s^{-1} at ambient temperature without external environment control. PBI specimens were cut according to ASTM D882 standard. The PA doping levels of PBI membranes were measured using a Metrohm 716 DMS Titrino Antomated Titrater with 0.01 M sodium hydroxide solution. The PA doping levels, X, were expressed as moles of PA per mole of PBI repeat unit (PA/RU) and calculated using Eq. (1). The V_{NaOH} and C_{NaOH} are the volume and concentration of sodium hydroxide required for the neutralization to reach the first equivalent point (EP1). The W_{dry} is the dry weight of polymer obtaining by drying the sample in oven at 110 °C overnight after titration. M_w is the molecular weight of the PBI repeat unit. Proton conductivities (σ) were measured through a four-probe AC impedance method using a Zahner IM6e electrochemical station with a frequency range from 1 Hz to 100 kHz and amplitude of 5 mV. A rectangular sample was cut from the membrane and placed in a polysulfone cell with four platinum electrodes. Both two outer electrodes and two inner electrodes were placed on opposite sides of the membrane to obtain through-plane membrane proton conductivity. A programmable oven was used to measure the proton conductivity at different temperatures and two conductivity runs were performed. In the first run, the temperature was raised to 180 °C to remove the water; in the second run, the data were collected for proton conductivity calculation according to the Eq. (2). The D is the distance between two inner electrodes. W and T stands for the width and thickness of the membrane, respectively. R is the impedance value measured.

$$X = \frac{V_{NaOH} \times C_{NaOH} \times M_w}{W_{dry}} \quad (1)$$

$$\sigma = \frac{D}{W \times T \times R} \quad (2)$$

2.4.3 Membrane Electrode Assembly (MEA) Fabrication and Fuel Cell Testing

The fuel cell gas diffusion electrodes with carbon cloth substrates and catalyst loading of 1.0 mg cm^{-2} (Anode: Pt; Cathode: Pt alloy) were acquired from BASF Fuel Cell, Inc. The MEA with an active area of 10.15 cm^2 was fabricated by quickly dipping the respective PA-doped membranes (24 μm thickness) into 85% PA bath for 10–20 s, placing between an anode electrode and a cathode electrode, and then directly hot pressing without shim at 140 °C and 6 N cm^{-2} for approximately 10 min. The MEA was then assembled into a single cell fuel cell testing hardware and the compression ratio of the MEA was controlled by gaskets to reach approximately 80–85%. Fuel cell performance testing was conducted by a commercial fuel cell testing station from Fuel Cell Technologies, Inc. Polarization curves were obtained from 120 °C to 180 °C with H_2/Air and H_2/O_2 as fuel/oxidant gases at a stoichiometric ratio of 1.2 and 2.0, respectively, without external humidification or back pressure.

3 Results and Discussion

3.1 Synthesis of 2,2′-bis(trifluoromethyl)-4,4′-biphenyldicarboxylic acid

The synthesis of 2,2′-bis(trifluoromethyl)-4,4′-biphenyldicarboxylic acid (**3**) was reported previously [22–24]. In the reported synthetic schemes, the key step is the preparation of a dinitrile intermediate (**2**), namely 2,2′-bis(trifluoromethyl)-4,4′-biphenyldicarbonitrile, by a metal-catalyzed aromatic coupling reaction. However, the preparation of the dinitrile precursor required multiple-step procedures and the coupling reaction provided relatively low yields and a large amount of by-products such as m-aminobenzotrifluoride, which could be caused by the existence of two strong electron-withdrawing groups (–CN, $–CF_3$) on a single reactant [24]. In this work, the synthesis of the diacid monomer was achieved through a simplified two-step method by using 2,2′-bis(trifluoromethyl)benzidine (**1**) as the starting material (Figure 1). Copper(I) cyanide was employed initially as the Sandmeyer cyanating reagent to transform the diamine to dinitrile but only gave a very low yield (15.2%). Therefore, a tetrahedral copper-cyano complex ($Na_3[Cu(CN)_4]$) was introduced and moderately improved the yield to 25.6% [25]. The reason for the low reaction yield is not clear and under further investigation. Hydrolysis of dinitrile to the diacid was accomplished readily in a high yield (82.7%).

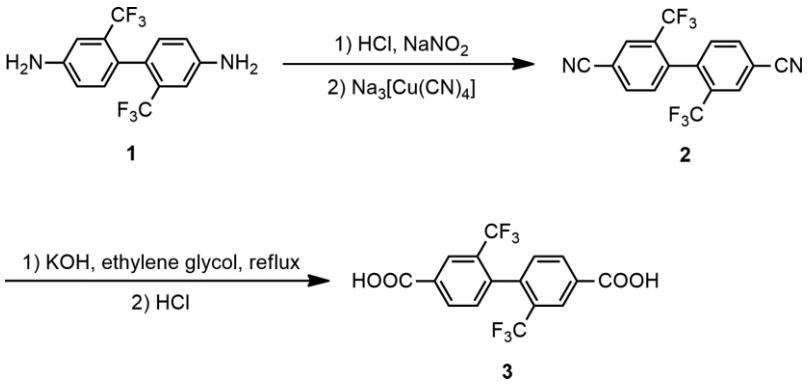

Fig. 1 Synthesis of 2,2′-bis(trifluoromethyl)-4,4′-biphenyldicarboxylic acid.

3.2 Synthesis of PBI Polymers

There are several strategies for the synthesis of PBI polymers such as melt polymerization and solution polymerization. A two-stage melt-solid polymerization method is currently applied for the production of commercially available *meta*-PBI. Another important synthetic approach is by solution polymerization in polyphosphoric acid (PPA). It is more favored for laboratory-scale study since it can be used as both solvent and condensation reagent and often produces high molecular weight polymers. Therefore, the solution polymerization of BTBP-PBI in PPA was also investigated early in this study. The diacid monomer exhibited good solubility in PPA at elevated temperatures. However, as the temperature rose to approximately 170 °C, the polymer solution turned into a gel-like mass within a few minutes, which could be caused by cross-linking of polymer. As partial evidence, the product could not be fully dissolved in concentrated sulfuric acid to obtain IV's *via* our standard methods.

Eaton's reagent (PPMA, phosphorous pentoxide: methanesulfonic acid = 1:10, w:w) was reported to be a convenient alternative to PPA for carrying out alkylation and acylation reactions on aromatic systems [20]. It also provides advantages over PPA such as lower viscosity and moderate reaction temperatures. Qian et al. [15] reported the utilization of PPMA for the polymerization of a novel fluorinated-PBI and high molecular weight products (IV = 1.55 dl g^{-1}) were obtained. Therefore, PPMA was also examined in this work and high molecular weight polymers were successfully produced (Figure 2). The following stepwise temperature control was used to ensure both monomers were fully dissolved before the polymerization: stir at 50 °C for 1 h, ramp to 100 °C over 6 h, stir at 100 °C for 18 h, ramp to 140 °C over 6 h, stir at 140 °C for 30–40 h. Polymerization conditions were then experimentally optimized and Figure 3 shows the effect of the monomer charge on the IV of BTBP-PBI at a final polymerization temperature of 140 °C. It was found that the IV of the polymer reached the maximum of 1.60 dl g^{-1} when the monomer concentration was approximately 1 mmol:5.5 ml (monomer:solvent). When the monomer concentration was too high, the solution was found to be too viscous for efficient stirring. In contrast, when the concentration was too low, step growth reaction was inhibited.

High molecular weight *meta*-PBI (1.39 dl g^{-1}) and 6F-PBI (1.07 dl g^{-1}) were also prepared by solution polymerization in PPA according to the literature [14, 21]. The general synthetic scheme and the structures of PBIs are shown in Figure 4.

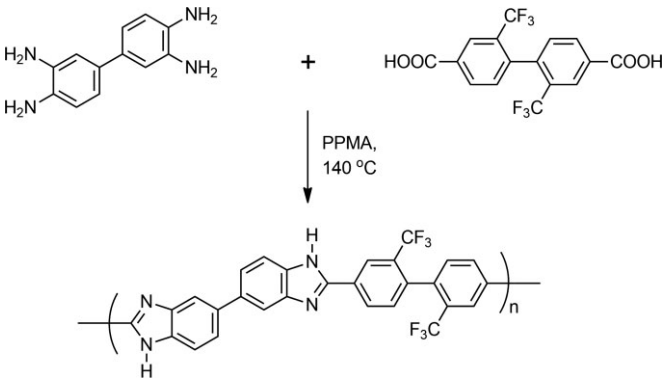

Fig. 2 Synthesis of BTBP-PBI in Eaton's reagent.

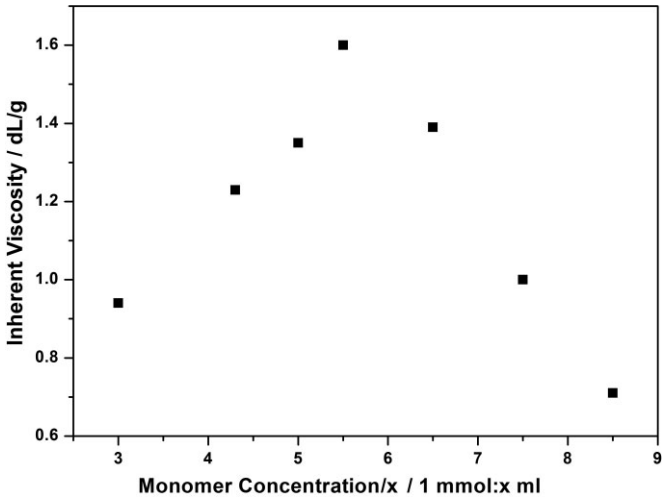

Fig. 3 Effect of monomer concentration on IV for BTBP-PBI at a polymerization temperature of 140 °C.

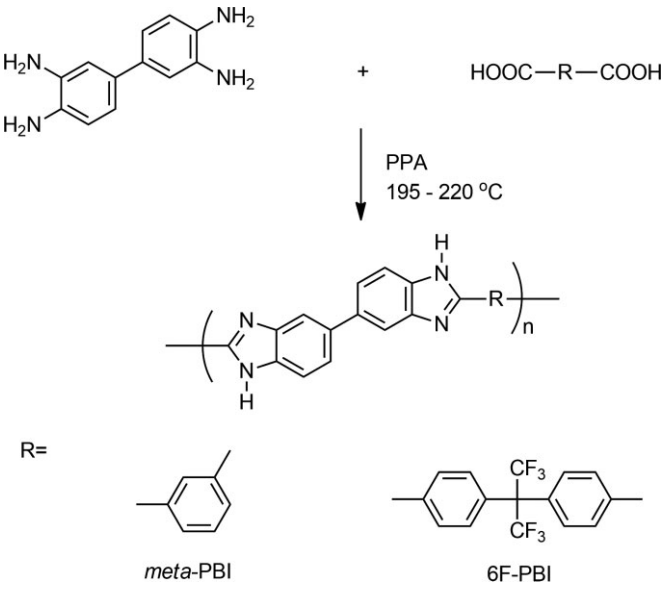

Fig. 4 Synthesis of *meta*-PBI and 6F-PBI in PPA.

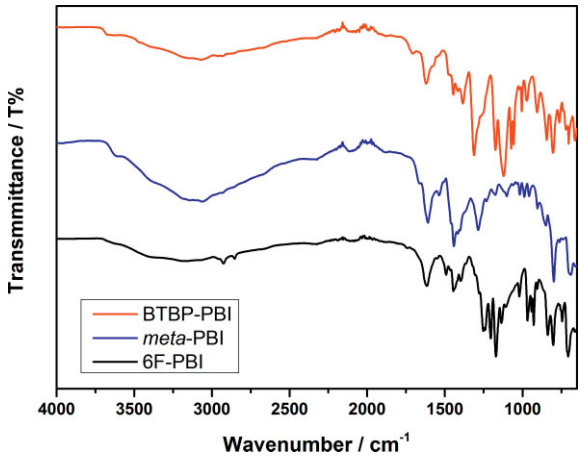

Fig. 5 FTIR spectra of BTBP-PBI, *meta*-PBI and 6F-PBI.

3.3 Polymer Characterization

3.3.1 Spectral Characterization

The BTBP-PBI as well as *meta*-PBI and 6F-PBI were characterized by FTIR and the spectra are shown in Figure 5. All polymers exhibited characteristic absorption bands in the broad region of 3500–2800 cm^{-1}, which are ascribed to the hydrogen bonded and non-hydrogen bonded N–H and aromatic C–H stretching of the benzimidazole rings. The region 1630–1380 cm^{-1} was attributed to the C=C and C=N stretching, in-plane ring vibration of benzimidazole as well as imidazole ring breathing mode. The broad peak at 1259–1313 cm^{-1} corresponded to the C–F stretching vibration of BTBP-PBI. The polymers were also characterized by ^{1}H NMR and ^{19}F NMR. In the ^{1}H NMR spectra (Figures 6–8), the benzimidazole characteristic proton signals were observed in all PBIs such as imidazole protons (e.g. for BTBP-PBI, H_4; 13.36 ppm) and biphenyl protons (e.g. for BTBP-PBI, H_1, H_2 and H_3; 7.68–8.07 ppm). In the ^{19}F NMR spectra (Figures 9 and 10), the fluorine signals of BTBP-PBI and 6F-PBI were observed at –57 ppm and –63 ppm, respectively. All the characterizations confirmed the successful preparation of the desired PBI polymers.

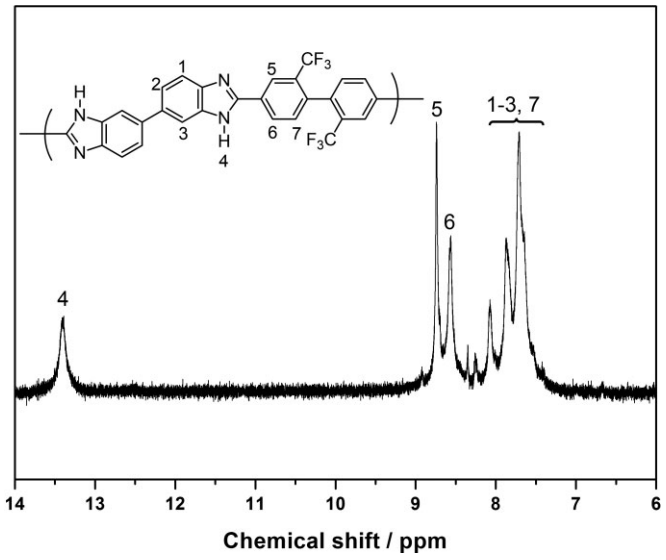

Fig. 6 ^{1}H NMR spectrum of BTBP-PBI in DMSO-d^6.

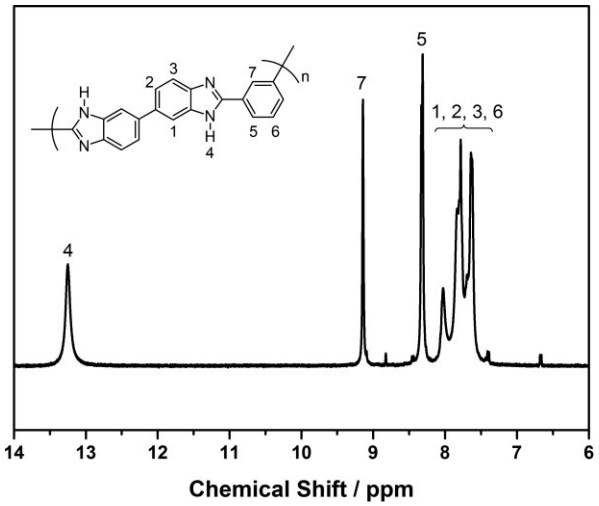

Fig. 7 ^{1}H NMR spectrum of *meta*-PBI in DMSO-d^{6}.

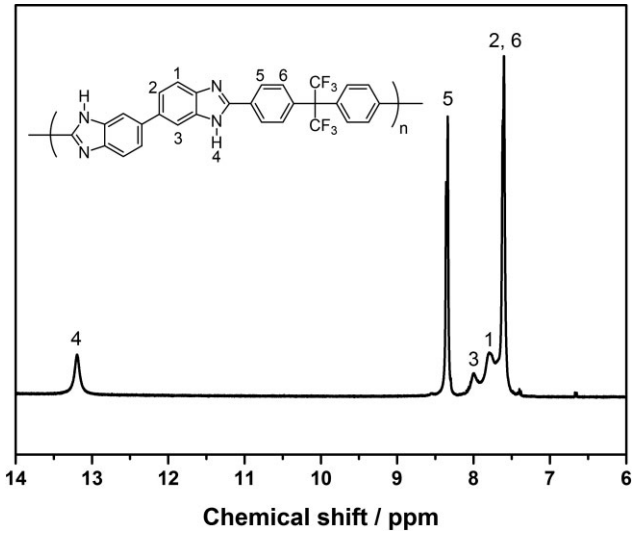

Fig. 8 ^{1}H NMR spectrum of 6F-PBI in DMSO-d^{6}.

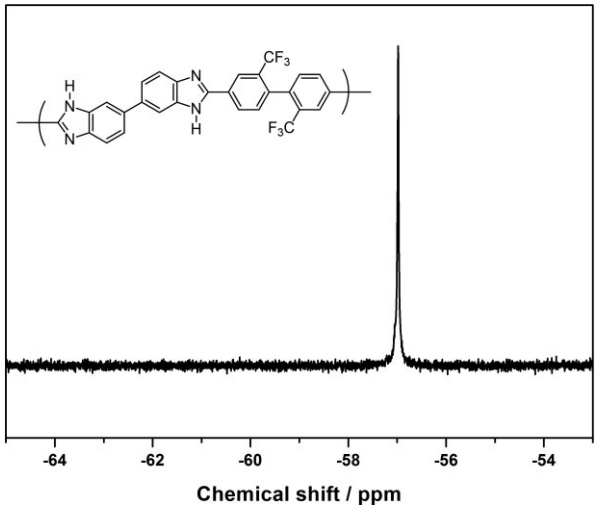

Fig. 9 ^{19}F NMR spectrum of BTBP-PBI in DMSO-d^{6}.

3.3.2 *Thermal Properties*

The thermal stability of BTBP-PBI, *meta*-PBI, and 6F-PBI were studied using TGA under nitrogen flow (20 ml min^{-1}) at a heating rate of 10 °C min^{-1} and the results are shown in Figure 11 and Table 1 (all of the weight loss calculations were based on the dry weight of polymers after water removal). The 7.0 wt.% water loss of BTBP-PBI between room temperature and ca. 200 °C was attributed to the hydrophilic characteristics of PBI polymers. This number is comparable to that of 6F-PBI (5.66 wt.%) but much smaller than that of *meta*-PBI (16.7 wt.%), which is likely caused by the introduction of the more hydrophobic trifluoromethyl groups. The BTBP-PBI

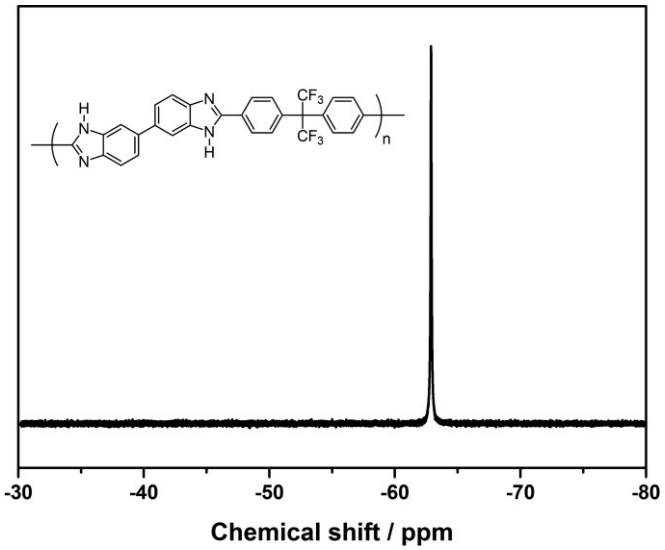

Fig. 10 ^{19}F NMR spectrum of 6F-PBI in DMSO-d^{6}.

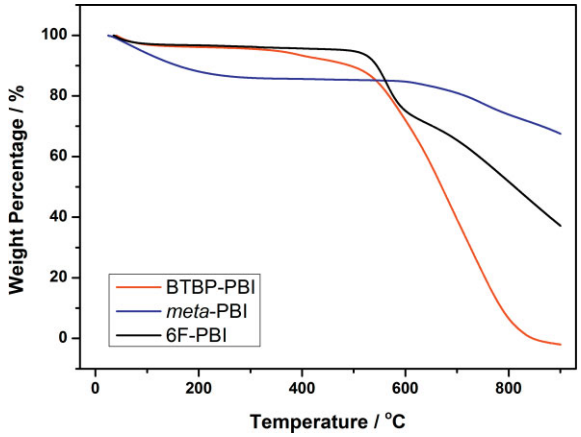

Fig. 11 TGA thermograms of BTBP-PBI, *meta*-PBI and 6F-PBI in nitrogen atmosphere.

Table 1 Thermal stabilities of PBI derivatives.

Polymer	Water (wt.%)	Decomposition temperature (°C)		
		0.02 wt.%	5.0 wt.%	10.0 wt.%
BTBP-PBI	7.00	277	471	536
meta-PBI	16.7	379	691	754
6F-PBI	5.66	410	478	566

was stable up to 277 °C (0.02 wt.% loss of the dry polymers) and the decomposition temperatures of TD_5 and TD_{10} (5 and 10 wt.% loss of the dry polymers) were 471 and 536 °C, respectively. The polymer was completely decomposed at 900 °C. The overall thermal stability of BTBP-PBI was slightly lower than that of *meta*-PBI and 6F-PBI, but sufficiently stable for realistic fuel cell applications [26]. The glass-transition temperature (T_g) of the BTBP-PBI was not detectable by DSC up to 450 °C.

3.3.3 Polymer Solubility

The solubility characteristics of all PBIs were determined at ambient conditions and at various polymer concentrations (1.0–5.0 wt.%) and the results are shown in Table 2. The BTBP-PBI polymer showed higher solubility than *meta*-PBI and comparable solubility as 6F-PBI in some polar, aprotic solvents such as DMAc, NMP, and DMF, which could be attributed to the introduction of the bulky and twisted biphenyl structure into the polymer backbone. However, it was found for the high concentration solutions (5.0 wt.%) that the BTBP-PBI polymers were susceptible to precipitating out of solution after sitting and formed gels. Further shaking at ambient conditions or slight heating did not convert it back to the solution state. The addition of LiCl (4 wt.%) to DMAc as a stabilizer effectively postponed or prevented the polymer precipitation. All polymers were insoluble in common organic solvents such as acetone, THF, and MeOH.

3.3.4 Oxidative Stability

The oxidative stabilities of all PBIs were investigated by measuring the weight loss of the pre-dried polymer powders, which had been immersed into Fenton's reagent for 24 h at different temperatures. Fenton's reagent (20 ppm Fe (II) in 3% H_2O_2) is an effective method to generate hydroxyl/peroxyl radicals to simulate the oxidative attack during the realistic fuel cell operation [27, 28]. Table 3 shows the testing results of BTBP-PBI as well as that of Nafion 115 and *meta*-PBI and 6F-PBI for comparison. It was found that the weight losses of BTBP-PBI at r.t. and 80 °C are 0 and 0.5 wt.%, respectively. This result is similar to that of 6F-PBI but lower than that of Nafion 115 and *meta*-PBI tested at similar conditions, indicating the trifluoromethyl groups are very stable from radical attack in harsh conditions.

3.4 Membrane Preparation and Characterization

3.4.1 PBI Dense Membrane Preparation

BTBP-PBI dense films were fabricated *via* a solution casting method. A 3.0 wt.% BTBP-PBI solution in DMAc was used for the initial film casting study. However, it was very difficult to obtain high-quality PBI dense films due to the short-term stability of the polymer solution as mentioned in Section 3.3.3. Therefore, a more dilute polymer solution (approximately 1.5 wt.%) was prepared and poured onto a glass plate with restraints on each side to obtain the dense films with desired thicknesses. When the wet film was dried in air, only opaque and mechanically weak films (Figure 12, left) were formed, indicating a strong phase separation, which could be attributed to the hydrophilic characteristics of both PBI and DMAc. In comparison, when the film was treated in a dry environment (dry nitrogen atmosphere), mechanically strong and transparent films (Figure 12, right) were successfully prepared. The *meta*-PBI and 6F-PBI films were prepared under similar optimized film processing conditions.

Table 3 Oxidative stability of PBI derivatives and Nafion tested in Fenton's Reagent for 24 h.

Sample	Weight loss%	
	r.t.	80 °C
Nafion 115	1.3	3.2
meta-PBI	0	0.8
BTBP-PBI	0	0.5
6F-PBI	0[a]	0 (180 °C)[a]

[a]The data was obtained from the literature [14].

Fig. 12 BTBP-PBI dense films (left: dried under air; right: dried under nitrogen).

Table 2 Solubility characteristics of PBI derivatives.

	DMAc		LiCl/DMAc		NMP		DMF		Acetone	THF	MeOH
	1.5 wt.%	5.0 wt.%	1.5 wt.%	5.0 wt.%	1.5 wt.%	5.0 wt.%	1.5 wt.%	5.0 wt.%	1.0 wt.%	1.0 wt.%	1.0 wt.%
BTBP-PBI	++	++*	++	++	++	++*	++	++*	–	–	–
meta-PBI	+	+	+	+	+	+	+	+	–	–	–
6F-PBI	++	++	++	++	++	++	++	++	–	–	–

DMAc, *N*,*N*-dimethylacetamide; LiCl/DMAc, 4 wt.% LiCl in DMAc; NMP, *N*-methyl-2-pyrrolidinone; DMF: *N*,*N*-dimethylformamide; THF, tetrahydrofuran; MeOH, methanol.
++, mostly soluble; ++*, mostly soluble, but polymer may precipitate from solution after sitting; +, partially soluble or swelling; –, insoluble.
meta-PBI and 6F-PBI were synthesized in house.

3.4.2 PBI Crystallinity

To study the polymer morphology of BTBP-PBI, the dense film prepared was examined using WAXS. Figure 13 shows the diffraction pattern of BTBP-PBI. A very broad peak (halo) was clearly observed, indicating the amorphous nature of polymer. It is believed that the introduction of twisted bistrifluoromethyl biphenyl groups effectively suppressed the polymer chain packing and crystallization. The polymer crystallinity of *meta*-PBI and 6F-PBI were reported in the literature and similar amorphous nature was observed [29]. The amorphous morphology is beneficial to improve the polymer's properties such as solubility and proton conductivity.

3.4.3 Acid Absorption

PA-doped BTBP-PBI membranes were prepared by immersing the dense films into PA solutions at ambient conditions for more than 48 h. The time for PBI membranes to reach maximum acid doping levels was reported to vary (16–50 h), which may be caused by variations in membrane thicknesses [30,31]. A series of PA baths with different concentrations (50% PA–90% PA) were used to study the polymers' acid absorption and stability behaviors. As shown in Figure 14, for BTBP-PBI, a steady increase in PA doping levels was observed with an increase in the PA bath concentrations until 75%. When the concentration reached 80%, the PA doping showed an abrupt increase to 10.70 PA/RU, which was caused by strong swelling of the polymer in acid. As evidence, a large increase of membrane thickness from 15 to 38 μm was observed. Beyond this PA concentration, the polymer membrane was found to be partially soluble. The 6F-PBI dense films were also dipped into PA solutions with similar concentrations to help to better understand how the PBI backbone structure could affect its acid uptake behavior. As shown in Figure 3, for 6F-PBI there are also two trifluoromethyl groups per polymer repeat unit within its backbone but these two groups are connected by a tetrahedral carbon center, which makes the polymer's backbone relatively more flexible than BTBP-PBI's. It was found these two PBIs exhibited similar doping behavior at low PA concentrations. However, 6F-PBI showed better stability and also a higher PA doping level when it was immersed in high concentration PA (approximately 13.17 PA/RU when soaked in 85% PA). This indicates that the more rigid polymer backbone and decreased chain flexibility of BTBP-PBI could result in the lower swelling ability as compared to 6F-PBI. The acid absorption behavior of *meta*-PBI was also reported and it showed slightly lower acid doping levels than the other two fluorinated PBIs.

3.4.4 Mechanical Properties

The tensile properties of BTBP-PBI dense membrane and the membranes with various PA doping levels were measured and the results are shown in Table 4. The pure PBI films showed a Young's modulus of 3.62 GPa, a tensile strength of 111 MPa and an elongation at break of 6%. These mechanical properties are higher than the other fluorine-containing PBIs that have been reported (e.g. the Young's modulus and tensile strength of 6F-PBI, 4F-PBI, and 14 F-PBI are all lower than 1.20 GPa and 55 MPa [12,16]). The mechanical properties of the membrane were reduced drastically when it was doped with PA and further decreased with increased PA doping levels, which is attributed to the increased plasticizing effect of the small molecules (PA and H_2O). The tensile properties of *meta*-PBI and 6F-PBI prepared in our lab were also tested and compared with that of BTBP-PBI as shown in Figures 15 and 16. They showed similar acid absorption trends and mechanical strength as BTBP-PBI. Figure 17 shows the composition percentages of BTBP-PBI membranes doped with different amounts of PA. It was found that as the PA doping level increased to 10.70 PA/RU the polymer percentage dropped to 22.50 wt.% whereas the percentages of acid and water increased to 45.35 and 32.14 wt.%, respectively. This is consistent with the large decrease in mechanical properties of the BTBP-PBI membranes. Similar trends were also observed from *meta*-PBI and 6F-PBI as shown in Figures 18 and 19.

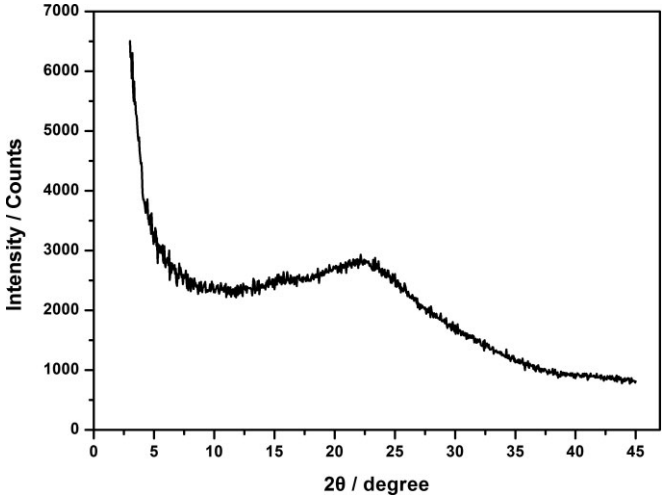

Fig. 13 WXRD pattern of BTBP-PBI dense film.

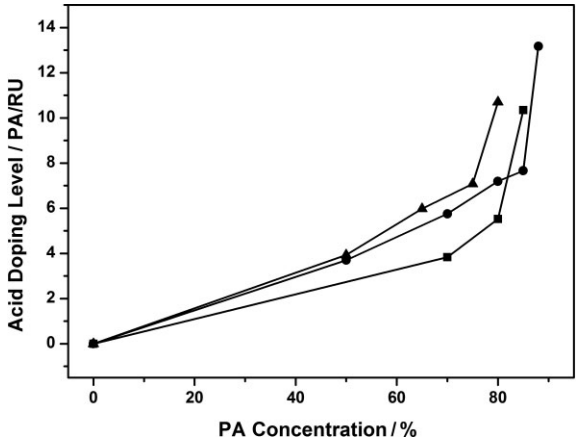

Fig. 14 PA doping levels of BTBP-PBI membranes (triangles), meta-PBI (squares) and 6F-PBI membranes (circles) treated by PA at different concentrations.

Table 4 Mechanical properties of BTBP-PBI membranes.

	Young's modulus (Gpa)	Tensile strength at break (MPa)	Tensile strain at break (%)
BTBP-PBI	3.617	111.3	6.225
BTBP-PBI – 3.93PA	1.446	46.43	12.58
BTBP-PBI – 5.98PA	0.664	26.59	29.13
BTBP-PBI – 7.08PA	0.394	14.52	30.25
BTBP-PBI – 10.70PA	0.069	3.264	36.19

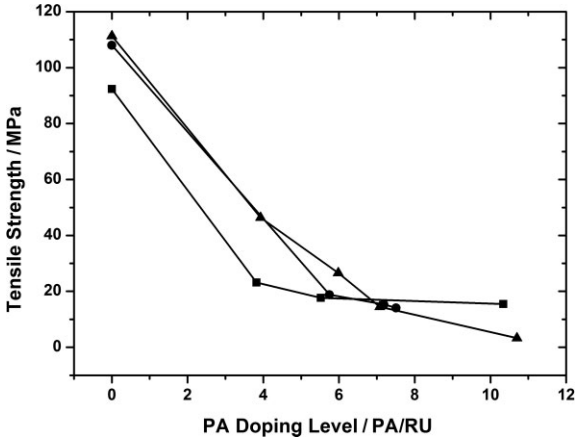

Fig. 15 Tensile Strength of PBI membranes (triangles: BTBP-PBI, squares: meta-PBI, circles: 6F-PBI) as a function of PA doping level at ambient temperature.

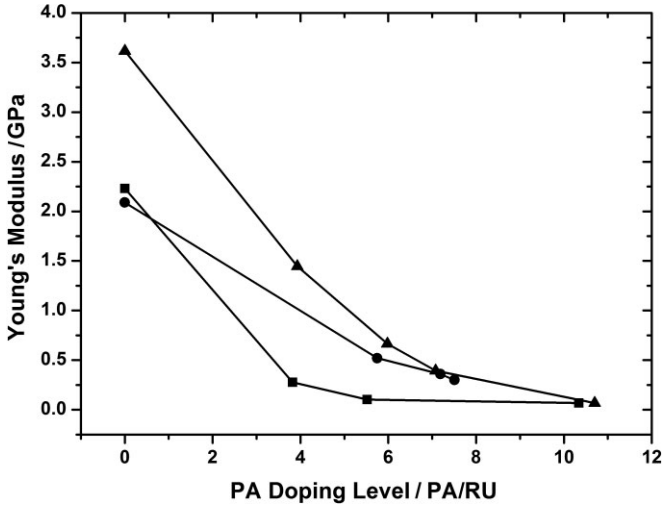

Fig. 16 Young's modulus of PBI membranes (triangles: BTBP-PBI, squares: meta-PBI, circles: 6F-PBI) as a function of PA doping level at ambient temperature.

3.4.5 *Proton Conductivity*

The proton conductivities of BTBP-PBI membranes with different PA doping levels were measured under anhydrous conditions as a function of temperature from r.t. to 180 °C. It was found that the conductivities increased with the increase in both temperature and acid loading. As shown in Figure 20, the conductivity values could be fitted by the Arrhenius equation (Eq. 3):

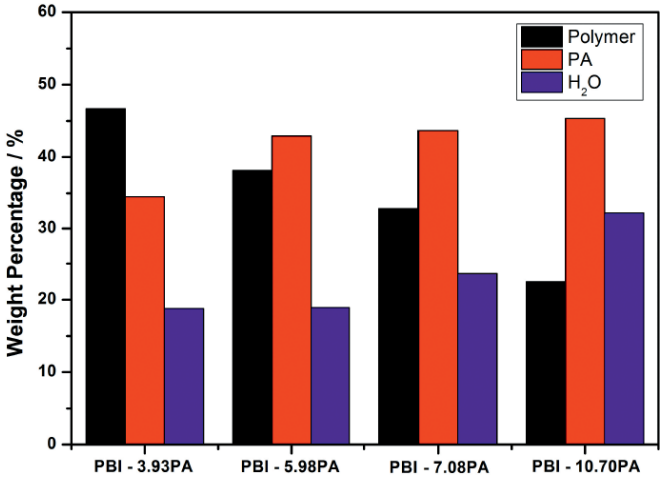

Fig. 17 Percentage composition of BTBP-PBI membranes treated by PA at different concentrations.

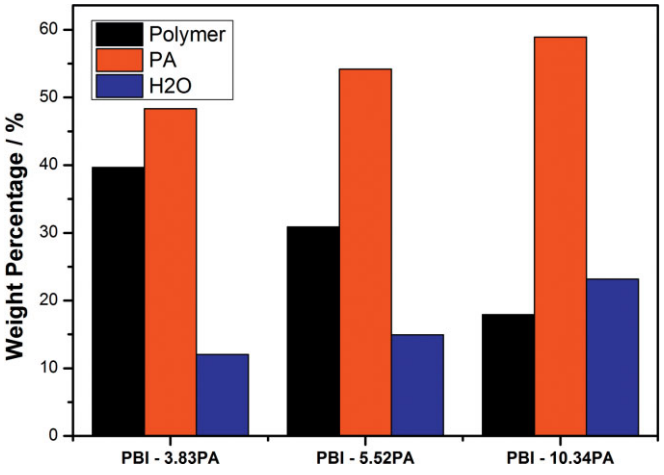

Fig. 18 Percentage composition of *meta*-PBI membranes treated by PA at different concentrations.

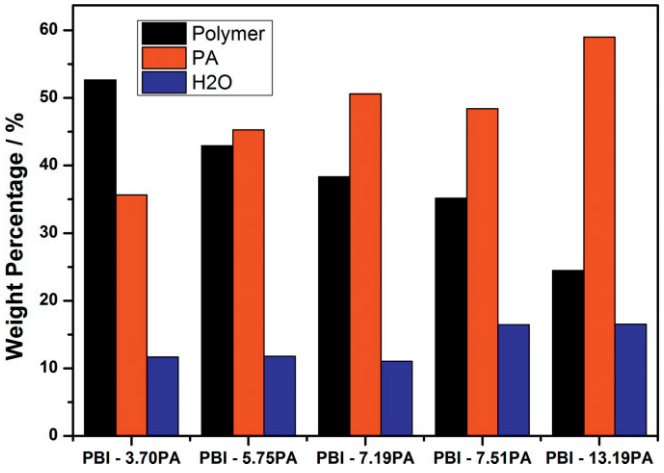

Fig. 19 Percentage composition of 6F-PBI membranes treated by PA at different concentrations.

$$\sigma = \sigma^0 \exp\left(\frac{-E_a}{RT}\right) = \frac{A}{T}\exp\left(\frac{-E_a}{RT}\right) \quad (3)$$

where σ^0 and A are pre-exponential factors; R is the Boltzmann constant; T is membrane testing temperature and E_a is the activation energy. The activation energy for proton conduction was found to decrease as the PA doping level increased (47.87 kJ mol^{-1} for doping level of 3.93 PA/RU; 46.58 kJ mol^{-1} for doping level of 5.98 PA/RU; 38.50 kJ mol^{-1} for doping level of 7.08 PA/RU). These values are of similar magnitude and trends to PA-doped *meta*-PBI membranes (41 KJ mol^{-1} for doping level of 3.00 PA/RU; 34 KJ mol^{-1} for doping level of 4.20 PA/RU; 27.5 KJ mol^{-1} for doping level of 6.0 PA/RU [32]). For the BTBP-PBI membrane with a doping level of 7.08 PA/RU, the maximum proton conductivity at 180 °C was approximately 0.02 S cm^{-1}, which is higher than literature data of some fluorine-containing PBI membranes (6F-PBI, 1.70 × 10^{-4} S cm^{-1}, 3.0 mol PA/RU, 160 °C [33]; 14F-PBI, 3.05 × 10^{-3} S cm^{-1}, 7.0 mol PA/RU, 150 °C [16]; 4F-PBI, ~6.31 × 10^{-4} S cm^{-1}, 7.0 mol PA/RU, 150 °C [16]) and also m-PBI (6.0 mol PA/PBI, ~1.0 × 10^{-2} S cm^{-1}, 160 °C, relative humidity = 0 [32]). It is noteworthy that the membrane with a PA doping level of 10.70 PA/RU (immersed in 80% PA) could not be tested accurately since it became very soft and underwent large deformation at elevated temperatures. In realistic fuel cell applications, it is important to find the best combination of proton conductivity and mechanical strength of the membrane.

3.4.6 *Fuel Cell Testing*

The BTBP-PBI membrane with a PA doping level of 7.08 PA/RU was chosen for the MEA preparation. Just prior to MEA fabrication, the membrane was dipped into a 85% PA solution for approximately 10–20 s, which was performed to decrease the interface resistance between membrane and electrodes. This acid pre-treatment was found to be effective in improving the ultimate fuel cell performance and the detailed mechanism is still under investigation. The fuel cell performance of BTBP-PBI was then investigated in a 10.15 cm^2 single cell fuel cell and Figure 21 shows the polarization curves of BTBP-PBI tested at 180 °C under H_2/Air and H_2/O_2. The open circuit voltages (OCV) of the membrane at both gas conditions were found to be low (0. 754 and 0.813 V under H_2/Air and H_2/O_2, respectively), which could be attributed to the relatively low membrane thicknesses (15 μm – before acid doping; and 24 μm – after acid doping) and non-optimized hot-pressing conditions (e.g. compression pressure, temperature, time, etc.). However, the membrane still operated reliably and, at a current density of 0.2 A cm^{-2}, the cell voltage of BTBP-PBI in H_2/Air operation was approximately 0.649 V. It then increased to 0.728 V when the gas pair was switched to H_2/O_2, which is due to the higher O_2 partial pressure at the cathode side. The maximum power densities that BTBP-PBI obtained under H_2/Air and H_2/O_2 were 0.462 and 0.574 W cm^{-2}, respectively. The overall fuel cell performance of BTBP-PBI was comparable to that of *meta*-PBI (190 °C, H_2/O_2, 0.55 W cm^{-2} at 1.2 A cm^{-2} [34]) and much better than that of 6F-PBI (160 °C, H_2/O_2, 0.43 W cm^{-2} at 1.0 A cm^{-2} [14]) reported in the literature.

4 Conclusion

A novel high molecular weight, thermally stable, and organo-soluble BTBP-PBI containing electron-withdrawing trifluoromethyl groups at the 2 and 2′ positions of a biphenyl moiety was successfully synthesized by solution polymerization in Eaton's reagent. A diacid, namely 2,2′-bis(trifluoromethyl)-4,4′-biphenyldicarboxylic acid, was synthesized and purified by a new simplified two-step method. The introduction of a tetrahedral copper-cyano complex ($Na_3[Cu(CN)_4]$) as cyanating reagent moderately increased the reaction yield

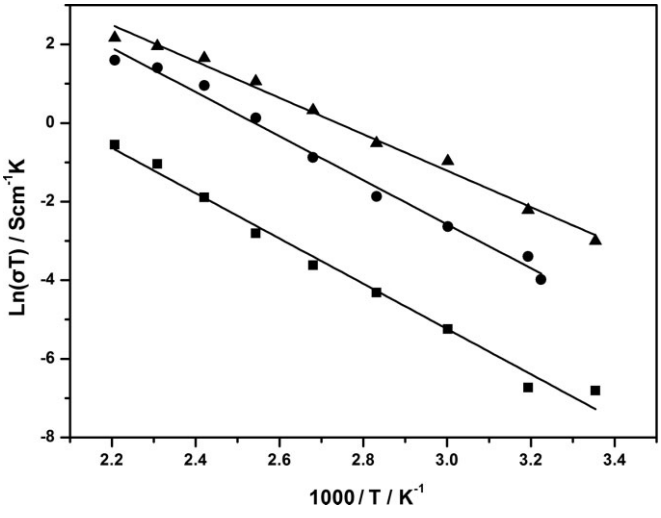

Fig. 20 Temperature dependence of proton conductivity of BTBP-PBI membranes without humidification. PA doping levels of PTBP-PBI membranes: (squares) 3.93 mole/RU; (circles) 5.98 mol/RU; (triangles) 7.08 mol/RU.

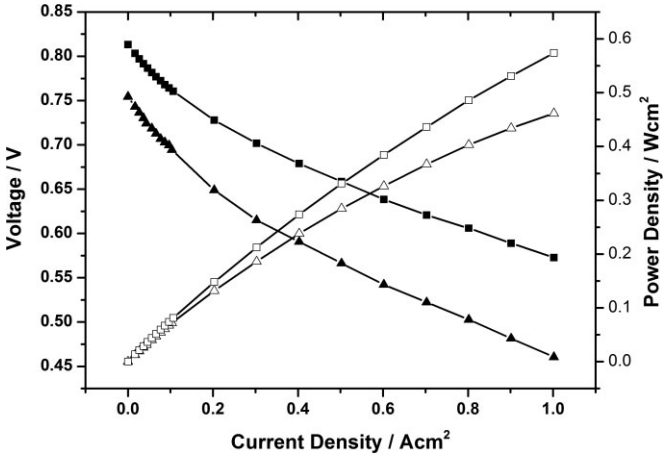

Fig. 21 Polarization curves (filled symbols) and power density curves (unfilled symbols) for MEA using BTBP-PBI membrane. (Fuel cell operation conditions: 1 atm, 180 °C, constant stoichiometry H_2 (λ = 1.2)/air (λ = 2.0) (triangles) or (λ = 1.2)/O_2 (λ = 2.0) (squares), no external humidification).

from 15.2 to 25.6%. Optimization of polymerization conditions to achieve high molecular weight polymers was explored by varying the initial monomer concentrations. The TGA results showed that the polymer had excellent thermal stability up to 471 °C (5 wt.% loss of dry polymer). The polymer exhibited good solubility in some polar, aprotic solvents such as DMAc due to the introduction of steric repulsion of the trifluoromethyl groups at the biphenyl moiety. Due to the presence of fluorine, the polymer also showed high resistance of hydroxyl/peroxyl radical attack in Fenton's reagent testing at both low and high temperatures. The PA-doped BTBP-PBI membranes were prepared by a traditional imbibing process. With increasing acid bath concentration, the PA doping levels of the membrane also increased whereas the mechanical properties decreased. It was found that BTBP-PBI membranes could be doped to 7.08 PA/RU in 75% PA solution and exhibit a proton conductivity of approximately 0.02 S cm^{-1}, which is higher than *meta*-PBI and some other fluorine-containing PBIs prepared by the same method and with similar doping levels. The MEA fabricated from the PA-doped BTBP-PBI membrane was tested in a fuel cell and showed approximately 0.65 V at 0.2 A cm^{-2} at 180 °C under H_2/Air, which is potentially useful in high temperature (120–200 °C) PEMFC applications.

Acknowledgement

The authors gratefully acknowledge the U.S. DOE/EERE-ITP for partial financial support of the project under contract CPS#18990.

References

[1] Q. Li, R. He, J. O. Jensen, N. J. Bjerrum, *Fuel Cells* **2004**, *4*, 147.
[2] R. Savinell, E. Yeager, D. Tryk, U. Landau, J. Wainright, D. Weng, K. Lux, M. Litt, C. Rogers, *J. Electrochem. Soc.* **1994**, *141*, L46.
[3] L. X. Xiao, H. F. Zhang, E. Scanlon, L. S. Ramanathan, E. W. Choe, D. Rogers, T. Apple, B. C. Benicewicz, *Chem. Mater.* **2005**, *17*, 5328.
[4] J. T. Wang, R. F. Savinell, J. Wainright, M. Litt, H. Yu, *Electrochim. Acta* **1996**, *41*, 193.
[5] S. R. Samms, S. Wasmus, R. F. Savinell, *J. Electrochem. Soc.* **1996**, *143*, 1498.
[6] S. Yu, H. Zhang, L. Xiao, E. W. Choe, B. C. Benicewicz, *Fuel Cells* **2009**, *9*, 318.
[7] M. G. Dhara, S. Banerjee, *Prog. Polym. Sci.* **2010**, *35*, 1022.
[8] S. Ando, *J. Photopolym. Sci. Technol.* **2004**, *17*, 219.
[9] K. Xie, J. G. Liu, H. W. Zhou, S. Y. Zhang, M. H. He, S. Y. Yang, *Polymer* **2001**, *42*, 7267.
[10] D. J. Liaw, K. L. Wang, *J. Polym. Sci. Pol. Chem.* **1996**, *34*, 1209.
[11] D. X. Yin, Y. F. Li, H. X. Yang, S. Y. Yang, L. Fan, J. G. Liu, *Polymer* **2005**, *46*, 3119.
[12] S. H. Hsiao, C. P. Yang, S. C. Huang, *J. Polym. Sci. Pol. Chem.* **2004**, *42*, 2377.
[13] S. Banerjee, G. Maier, R. Burger, *Macromolecules* **1999**, *32*, 4279.
[14] G. Qian, B. C. Benicewicz, *J. Polym. Sci. Pol. Chem.* **2009**, *47*, 4064.
[15] G. Qian, D. W. Smith Jr, B. C. Benicewicz, *Polymer* **2009**, *50*, 3911.
[16] H. T. Pu, L. Wang, H. Y. Pan, D. C. Wan, *J. Polym. Sci. Pol. Chem.* **2010**, *48*, 2115.
[17] R. A. Gaudiana, R. A. Minns, R. Sinta, N. Weeks, H. G. Rogers, *Prog. Polym. Sci.* **1989**, *14*, 47.
[18] H. G. Rogers, R. A. Gaudiana, R. A. Minns, *US Patent, US 4, 628, 125*, **1986**.
[19] H. G. Rogers, R. A. Gaudiana, R. A. Minns, *US Patent, US 4, 433, 132*, **1984**.
[20] P. E. Eaton, G. R. Carlson, J. T. Lee, *J. Org. Chem.* **1973**, *38*, 4071.
[21] H. Zhang, *Ph.D. Thesis*, Rensselaer Polytechnic Institute, New York, USA, **2004**.
[22] J. C. Chen, C. J. Chiang, Y. C. Liu, *Synth. Metals* **2010**, *160*, 1953.
[23] H. G. Rogers, R. A. Gaudiana, W. C. Hollinsed, P. S. Kalyanaraman, J. S. Manello, C. McGowan, R. A. Minns, R. Sahatjian, *Macromolecules* **1985**, *18*, 1058.
[24] N. Yonezawa, T. Namie, T. Ikezaki, T. Hino, H. Nakamura, Y. Tokita, R. Katakai, *React. Funct. Polym.* **1996**, *30*, 261.
[25] N. Yonezawa, T. Hino, T. Namie, R. Katakai, *Synth. Commun.* **1996**, *26*, 1575.
[26] A. S. Buckley, D. E. Stuetz, G. A. Serad, *Encycl. Polym. Sci. Eng.* **1987**, *11*, 572.
[27] E. Graf, J. R. Mahoney, R. G. Bryant, J. W. Eaton, *J. Biol. Chem.* **1984**, *259*, 3620.
[28] V. A. Sethuraman, J. W. Weidner, A. T. Haug, L. V. Protsailo, *J. Electrochem. Soc.* **2008**, *155*, B119.
[29] A. Carollo, E. Quartarone, C. Tomasi, P. Mustarelli, F. Belotti, A. Magistris, F. Maestroni, M. Parachini, L. Garlaschelli, P. P. Righetti, *J. Power Sources* **2006**, *160*, 175.
[30] S. Kumbharkar, M. N. Islam, R. Potrekar, U. Kharul, *Polymer* **2009**, *50*, 1403.
[31] Q. Li, R. He, R. W. Berg, H. A. Hjuler, N. J. Bjerrum, *Solid State Ionics* **2004**, *168*, 177.
[32] Y. L. Ma, J. S. Wainright, M. H. Litt, R. F. Savinell, *J. Electrochem. Soc.* **2004**, *151*, A8.
[33] S. W. Chuang, S. L. C. Hsu, *J. Polym. Sci. Pol. Chem.* **2006**, *44*, 4508.
[34] Q. Li, H. A. Hjuler, N. J. Bjerrum, *J. Appl. Electrochem.* **2001**, *31*, 773.

